



CHARACTERIZATION OF PRODUCED BIODEGRADABLE BRAKE-PAD FROM WASTE COCONUT FRUIT FIBER AND OYSTER SEA SHELLS AS REINFORCEMENT MATERIALS

* Eziwhuo SJ¹, Ossia CV², Joseph T³

¹Department of Mechanical Engineering, Federal Polytechnic Kaduna, Kaduna, Nigeria

²Department of Mechanical Engineering, University of Port Harcourt, Port Harcourt, Nigeria

³Department of Mechanical Engineering, Federal Polytechnic of Oil and Gas Bonny, Rivers State, Nigeria

ABSTRACT

In the present research, organic materials (coconut fruit fibres CFF and oyster sea shells OSS) were used as a substitute for asbestos materials. The waste CFF and OSS were washed, crushed, grounded, and sieved to different sizes. The sieved CFF and OSS as reinforcement materials were prepared in three different levels, K1, K2, and K3, with additive such as phenolic resin, graphite, copper, and hardener. Level K1 has 50% of OSS and 0% of CFF, K2 has 50% of CFF and 50% of OSS, while K3 has 50% of CFF and 0% of OSS. The prepared levels were moulded in clean metal moulding plates up to twenty-seven (27) runs using the Box Behnken Design technic of four factors and three levels. The 27 produced brake pads and commercial brake pad CBP were tested in a laboratory to determine their characterization, such as; thermal conductivity, thermogravimetric analysis (TGA) and wear rate. The characterization of the produced brake pad has a related standard brake pad coefficient of friction of 0.3 – 0.45 while that of produced brake pad PBP has the lowest TGA of S3232 - 25.44% than CBP 41.90% and PBP of S3122 has the lowest wear rate of 3.17 than CBP 3.92g. From the evaluation, the PBP were superior and performed best in braking application.

Keywords: *thermogravimetric analysis; coefficient of friction; wear rate, coconut fruit fiber; oyster sea shell*

1. Introduction

Asbestos has been used as a major reinforcement material in producing commercially marketed brake pads because of its high thermal conductivity, wear resistance capacity, high thermal stability, and low cost. However, the US Environmental Protection Agency in 1986 proposed a ban on asbestos material due to its carcinogenic nature. Hence, from the researchers again, Europe has regulated against harmful ingredients used in some raw materials like commercial friction lining materials, which could have an impending undesirable ecosystem effect. The main purpose of the suggested ban was to stop the industry from manufacturing brake pads through asbestos materials and other friction lining constituents and boost the use of organic, eco-friendly materials [1]. Different materials that makeup automobile brake pads are classified as fillers (reinforcement/base materials), friction modifiers, binders, and abrasives [2]. Brake pads are critical safety mechanisms for moving vehicles to relaxation by translating kinetic energy to heat energy and engaging the heat to the surroundings by high

thermal conductivity. Besides human health and eco-friendliness, brake lining primary functions include low resistance to wear, low absorption rate, low weight, good friction, high compressive strength, rigidity, hardness, thermal stability, thermal conductivity, etc. This research was accomplished experimentally, and the outcomes of the produced brake pad were investigated and linked with the equivalent results of a commercial market brake pad material.

Good brake pads are organic friction lining materials since the matrix of these complex combinations is made by one or other polymers [3-4]. Available commercial automobile brake pads are approximately categorized in place of low metal, semi-metal, and organic materials. At the same time, producing better friction material is to find the greatest stability among the numerous factors producing low cost, acceptable performance and environmentally friendly (ecofriendly). Some additive materials discussed [5-6] in brake pad includes; epoxy resin, phenolic resin, carbide, aluminum, antimony, silicon, tri-sulfide, lead, copper, graphite, potassium, tin, titanate, whisker, aramid, and more. But this research

*Corresponding Author - E-mail: ufuomaluv@gmail.com

used copper, phenolic resin, hardener, and graphite as substitutes.

2. Materials and Methods

2.1 Materials

The materials used in this research work include:

- (a) Oyster Sea Shell (OSS) (Reinforcement),
- (b) Coconut Fruit Fiber (CFF) (Reinforcement),
- (c) Graphite (Friction Modifier),
- (d) Copper Oxide (Abrasive),
- (e) Phenolic Resin (Binder),
- (f) Hardener (Catalyst).

2.2 Equipment and materials

The equipment and materials used for this friction lining production are;

- i. Manual Compression Molding Machine. – Source from Civil Engineering Laboratory, University of Port Harcourt, Port Harcourt Rivers State.
- ii. Vernier calliper Model; 530-105 - Source from Mechanical Engineering workshop, University of Port Harcourt, Port Harcourt Rivers State
- iii. Weighing Machine. OHAUS, S/N B43391, Made in USA, Readability: 0.0001g – Source from School of Science Laboratory Technology (SSLT), University of Port Harcourt, Port Harcourt Rivers State.
- iv. Electric Oven – Saisho – 5000W, Made in China, Model: S-936R, S/N: S936R-SA1811120TO00899. SOURCE: Personal.
- v. Oxford Instrument X-Met 7000 XRF Spectrometer, Energy Dispersive X-Ray Fluorescence Analysis (ED-XRFA) Methodology. Wire brushes, industrial rags. Source - Turret Engineering Services Ltd Port Harcourt Rivers State Nigeria.
- vi. Electric Crushing Machine.- Source from Civil Engineering Laboratory, University of Port Harcourt, Port Harcourt Rivers State.
- vii. Sieving Mesh Aperture. - Source from Civil Engineering Laboratory, University of Port Harcourt, Port Harcourt Rivers State.
- viii. The Perkin-Elmer TGA 7 Thermo Gravimetric Analysis (TGA). Source- Centre for Genetic Engineering and Bio-Technology (STEP B) in the Federal University of Technology, Minna.
- ix. Inclined plane (Model No. 14678; NORWOOD Instrument Ltd.). Source- Mechanical

workshop, Federal University of Technology, Minna.

- x. SAE 40 lubricating oil (Oando).



Fig. 1 Waste Coconut fruit fiber (*Coir L.*) and Oyster Sea shell (*Magallana-Gigas L.*)

2.3. Formulation of Different Based Samples

The based / reinforcement materials (Coconut Fruit Fiber CFF and Oyster Sea Shell OSS) and supplementary additive (copper chips were abrasives materials that boost the thermal stability and conductivity, Phenolic resin was binder materials, graphite was friction modifier, and hardener was a catalyst) were produced by using published literature [7-8] that has standard processes. The OSS and CFF were equipped for the moulding of Brake-lining in three different levels (K1, K2, and K3) (Figure 1.). All the production samples (based / reinforcement materials and additive) were mixed thoroughly until a rise of standard intensification processes was formulated and put into an already cured circular moulding plate. Forming started with hotness, as it was permitted to stay for three minutes, which proved an exothermic reaction. After the reaction, moulding pressure P_m was mounted for two hours with different parameters upon which complete curing had taken place and instantly relocated to an electric machine oven with different values of moulding temperature T_m and heat treatment time T_{ch} (see Table 1).

Table 1 Brake-lining Materials Composition

Lining Material	Level K1(G)	Level K2(G)	Level K3(G)
Hardener	18	18	18
Graphite	4.5	4.5	4.5
Phenolic	31	31	31
Copper	4.5	4.5	4.5
Cff	72	36	0
Oss	0	36	72
Total	130	130	130

Table 2 Different factors and levels

Levels	Lower (-1)	Middle (0)	Upper (+1)
Filler Material	K1 (0 CFF /100 OSS)	K2 (50 CFF /50 OSS)	K3 (100 CFF /0 OSS)
Moulding Pressure, P _m (KPa)	14	16	18
Moulding Temperature, T _m (°C)	80	120	160
Heat Treatment Time T _{ht} (min)	50	100	150

2.4 Experimental Design

For this researched work, Box Behnken design of experiment was used; since it contains four factors (using Reinforcement Materials (RM), Molding Temperature (T_m), Molding Pressure (P_m), and Heat Treatment Time (T_{ht}) and three-level (lower -1, middle 0, and higher +1) design (shown in Table 3).

Table 3 Four Factors and Three Levels of Box – Behnken Design Experiment

S/N.	Reinforcement Material	P _m (Pa)	T _m (°C)	T _{ht} (minute)
1	K1	14	80	50
2	K3	18	160	150
3	K1	14	80	50
4	K3	18	160	150
5	K2	16	120	100
6	K2	16	120	100
7	K2	16	120	100
8	K2	16	120	100
9	K1	14	80	50
10	K3	18	160	150
11	K1	14	80	50

12	K3	18	160	150
13	K2	16	120	100
14	K2	16	120	100
15	K2	16	120	100
16	K2	16	120	100
17	K1	14	80	100
18	K3	18	160	150
19	K1	14	80	50
20	K3	18	160	150
21	K2	16	120	100
22	K2	16	120	100
23	K2	16	120	100
24	K2	16	120	100
25	K2	16	120	100
26	K2	16	120	100
27	K2	16	120	100

2.5 Characterization of produced lining samples

The produced lining samples were verified in directive to assess the thermogravimetric analysis TGA, friction coefficient, and wear rate with commercial friction lining. This assessment was characterized using the standard testing machine arrangement method.

2.5.1 Thermogravimetric Analysis (TGA) Test

The equipment TGA used was Perkin-Elmer TGA 7. The thermogravimetric (TG) refers to the amount of weight changes when a sample is heated to a programmed heating. In general, TG involves measuring weight loss as a function of temperature. The temperature range was 30°C - 800°C at a heated rate of 12°C/min. The accurate mass measurement (1 – 10mg) and ideal sample weight range (1–10g). The data acquisition system and heating control computer-based system were all connected to the furnace of thermogravimetric and cooling the furnace with liquefied nitrogen. A flow rate of 27 ml/minute) at the atmosphere of air were used (Table 4) in that order.

2.5.2 Coefficient Of Friction

2.5.2.1 Static Coefficient

The brake pad produced was placed on the incline plane and the angle of inclination increased until the pad fairly activated to slip down the surface. The height, h, and resultant to this slope was measured. The length of the inclined plane, x was constant. The computed coefficient of friction for friction lining samples under dissimilar situations are seen in Table 5.



Fig. 2 Inclined plane

2.5.2.2 Dynamic Coefficient

First, small nylon was used to grip the produced brake lining lightly and engaged on a sophisticated metal plate. As a frictionless component, the pulley groove was tied to a load hanger. A weight of 1200g was placed on the produced lining, with the pad weight in grams times 9.81 m/s^2 giving a normal load. Again the load hook was increasingly loaded, upon each filling, the friction lining was casually selected, and a steady slow velocity was notified through the weight. The weight of the load hanger (120g) with weight notified through velocity multiplied by 9.81 m/s^2 gives frictional load. The coefficient of dynamic friction results were shown (see Table 5).

2.5.3 Wear rate analysis

The equipment used in this test were automobile wheel discs of an inner diameter of 175mm and outer diameter of 292 mm; a lathe machine; plain spring compression dimensions of an outer diameter of 28mm, inner diameter of 25mm, and 53 mm long. Produced brake pad holders were used in devising a friction testing machine. The wheel disc contact face was made in the USA, with aluminium silicon grit No. q-500C, emery paper, bonded together. The disc wheel was lightly gripped in the chuck of the lathe machine running at 150rpm. The produced brake lining was placed in the pad holder contrary to the spring and forced into the emery paper to compression spring. Based on compression spring parameters and pad interaction area, 74 KN/m^2 was given to disc/linings pressure that ran at a time of 18 minutes. The wear of lining weight was measured after and before the test, respectively (see Table 6).

3. Result and Discussion

3.0 Thermogravimetric Analysis

Thermogravimetric Analysis (TGA) refers to the measurement of weight changes when a sample is heated to a slated heating platform. In general, TGA involves the measurement of weight loss as a function of temperature. Thermal stability is the efficacy of a fluid to deny it breaking down under heat pressure or thermal Stability is the decomposition of a compound on heating. The thermal stability of S3232 – 25.44% and S2222 – 25.84% samples was confirmed by Figure 6 and 4.9e thermogravimetric analysis TGA chart at a temperature of 800°C . The thermogravimetric analysis TGA data (Figure. 3. – 8.) show weight loss of all twenty-seven produced brake pad PBP samples and commercial brake pad CBP as a function of temperature. All the lining samples start losing their weight above 30°C , which can be attributed to the thermal degradation of "organic constituents," including hardener, phenolic resin, copper oxide, and graphite. Oxidation and decomposition of the carbonaceous substance linger up to 800°C , and burnt organic mechanisms and copper and graphite reaction with existing oxygen. Oxidizing metals during heating in thermogravimetric analysis TGA is one of the potential reasons that the produced brake pad samples with the peak metal content (copper oxide) demonstrate the greatest seeming thermal stability in the thermogravimetric analysis TGA investigation. The weight of the samples increases as metal (copper oxides) forms, while produced friction lining samples lose their masses when organic constituents oxidize or decompose.

3.1 Coefficient Of Friction

Figures (9 –14) show that shows the characterized coefficient of friction obtained from friction pads and control pads varies with the composition of materials used in the production. The friction coefficient of brake lining as a function of speed changes as it is imperative to drivers who expect the same level of friction force in several situations [9], and the friction coefficient of materials varies as the mass changes. From observation, in an ideal dry condition, the dynamic coefficient of friction obtained was less than the static coefficient of friction. The friction coefficient values for samples S2132 dry static coefficient of friction 0.458, and S2312 SAE40 coefficient of friction (0.30) agreed with the values of 0.3–0.46 reported by [10]. They were superior to the value of SAE-40 dynamic coefficient of friction 0.318 obtained from commercial control brake lining. The variation coefficient of friction detected may be due to

copper oxide fibers [10] testified that copper oxide fibers play a major role in improving the coefficient of friction. Continuous friction coefficient increase is habitually accompanied by the grip of metal chips in the brake lining to the friction surface. [11] The variation could also be credited to the developing rupture of asperities and cold welding of virgin friction pad surfaces. Hence, there is no cause for an over-increase in the coefficient of friction due to no isolated asperities

trapped between the sliding surfaces. Definite oxides have characteristics of lubricating and could help the solid lubricant additives already included in the friction pad production to minimize the friction further.

The result achieved is better than the values obtained from the control brake pad, and the coefficient of friction of the dynamic and static friction pads produced do fall within the industrial standard choice of 0.3 to 0.45 for vehicle brake pad [12],

Table 4 Thermogravimetric analysis

S/N.	TGA (wt.%)	Init. T 30 °C	Tem. 100 °C	Tem. 200 °C	Tem. 300 °C	Temp. 400 °C	Temp. 500 °C	Temp. 600 °C	Temp. 700 °C	Temp. 800 °C
1	S1122	100	97.48	87.48	77.48	67.48	57.48	47.48	37.48	27.48
2	S3122	100	95.65	86.65	77.65	68.65	59.65	50.65	41.65	32.65
3	S1322	100	99.10	89.10	79.10	69.10	59.10	49.10	39.10	29.10
4	S3322	100	96.82	90.32	83.82	77.32	70.82	64.32	57.82	51.32
5	S2211	100	99.55	91.55	83.55	75.55	67.55	59.55	55.55	43.55
6	S2231	100	98.66	93.96	89.26	84.56	79.86	75.16	70.46	65.76
7	S2213	100	96.92	86.92	76.92	66.92	56.92	46.92	36.92	26.92
8	S2233	100	98.61	88.61	78.61	68.61	58.61	48.61	38.61	28.61
9	S1221	100	94.10	86.10	78.10	70.10	62.10	51.10	46.10	38.10
10	S3221	100	94.22	85.22	76.22	67.22	58.22	49.22	40.22	31.22
11	S1223	100	97.46	87.46	77.46	67.46	57.46	47.46	37.46	27.46
12	S3223	100	98.77	92.77	86.77	80.77	74.77	68.77	62.77	56.77
13	S2112	100	94.35	87.35	80.35	73.35	66.35	59.35	52.35	45.35
14	S2312	100	93.90	84.90	75.90	66.90	57.90	48.90	39.90	30.90
15	S2132	100	97.84	92.84	87.84	82.84	77.84	72.84	67.84	62.84
16	S2332	100	96.51	89.51	82.51	75.51	68.51	61.51	54.51	47.51
17	S1212	100	98.33	88.33	78.33	68.33	58.33	48.33	38.33	28.33
18	S3212	100	96.97	86.97	76.97	66.97	56.97	46.97	36.97	26.97
19	S1232	100	96.91	87.91	78.91	69.91	60.91	51.91	42.91	33.91
20	S3232	100	95.44	85.44	75.44	65.44	55.44	45.44	35.44	25.44
21	S2121	100	97.98	87.98	77.98	67.98	57.98	47.98	37.98	27.98
22	S2321	100	96.39	90.79	85.19	79.59	73.99	68.39	62.79	57.19
23	S2123	100	96.9	92.2	87.5	82.8	78.1	73.4	68.70	64.00
24	S2323	100	98.77	90.77	82.77	74.77	66.77	58.77	50.77	42.77
25	S2222	100	95.84	85.84	75.84	65.84	55.84	45.84	35.84	25.84
26	S2222	100	95.84	85.84	75.84	65.84	55.84	45.84	35.84	25.84
27	S2222	100	95.84	85.84	75.84	65.84	55.84	45.84	35.84	25.84
28	CBP %	100	97.90	89.90	81.90	73.90	65.90	57.90	49.90	41.90

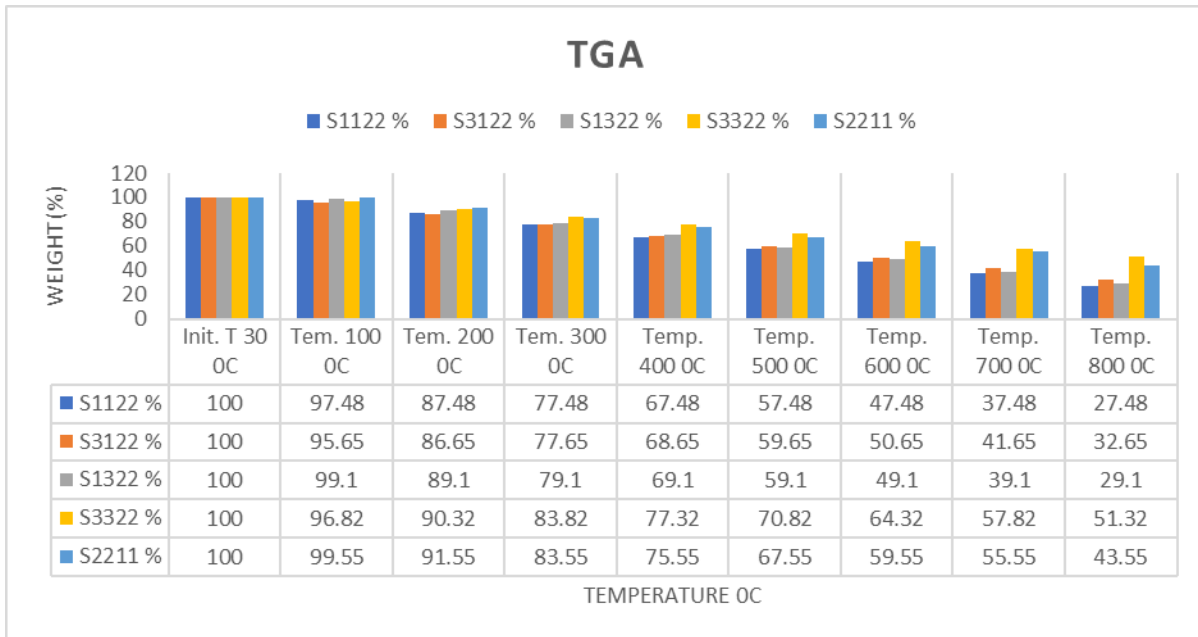


Fig. 3 TGA chart of S1122, S3122, S1322, S3322, and S2211 with variation of temperatures

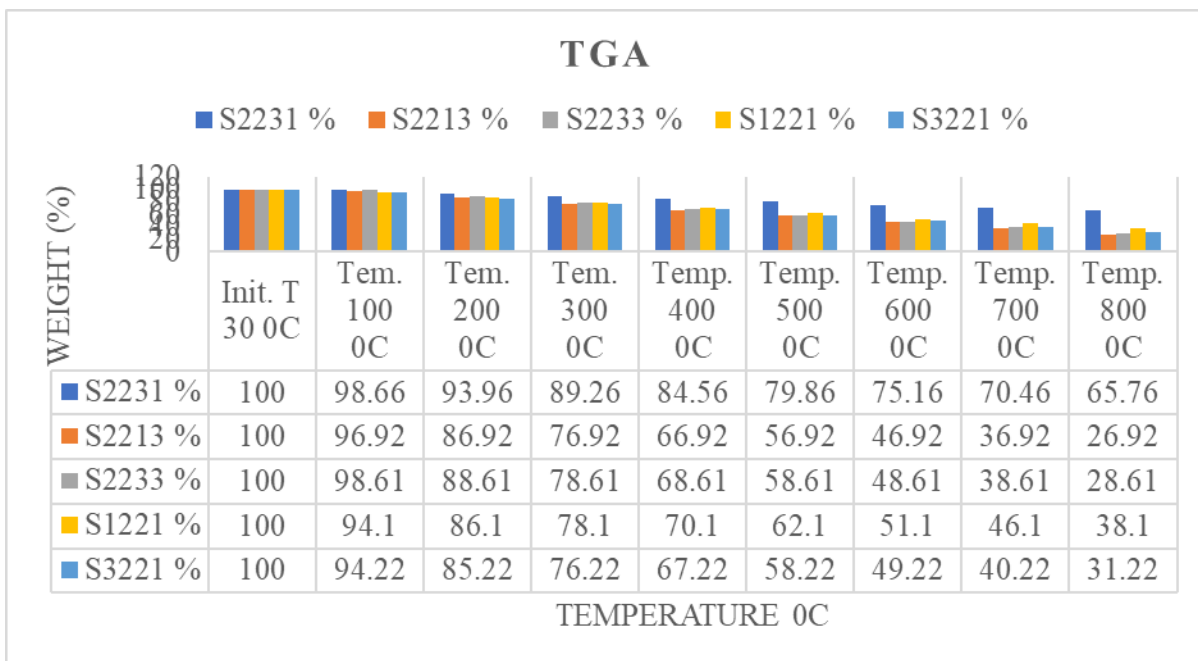


Fig. 4 TGA chart of S2231, S2213, S2233, S1221, and S3221 with variation of temperatures

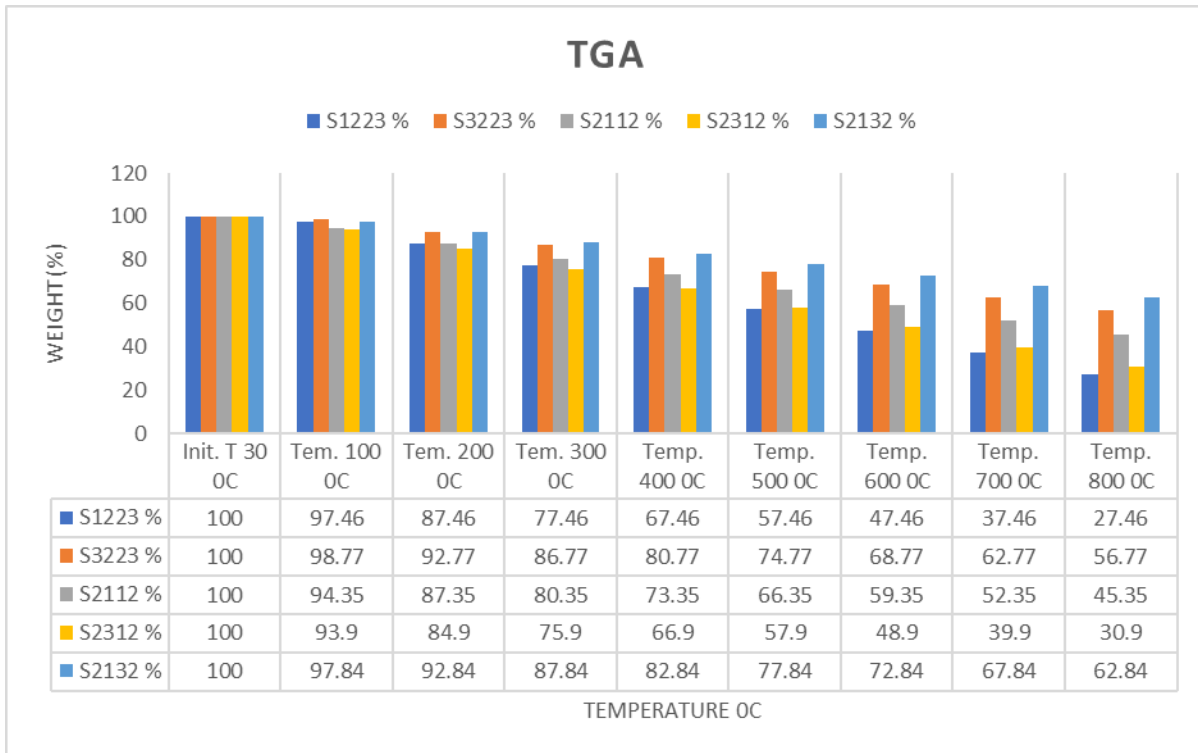


Fig. 5 TGA chart of S1223, S3223, S2112, S2312, and S2132 with variation of temperatures

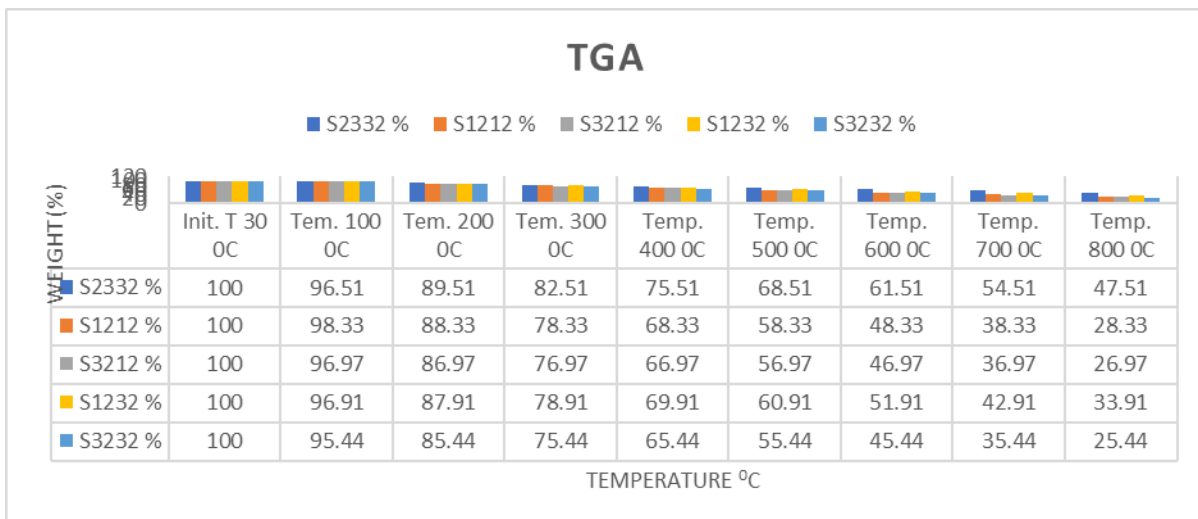


Fig. 6 TGA chart of S2332, S1212, S3212, S1232, and S3232 with variation of temperatures

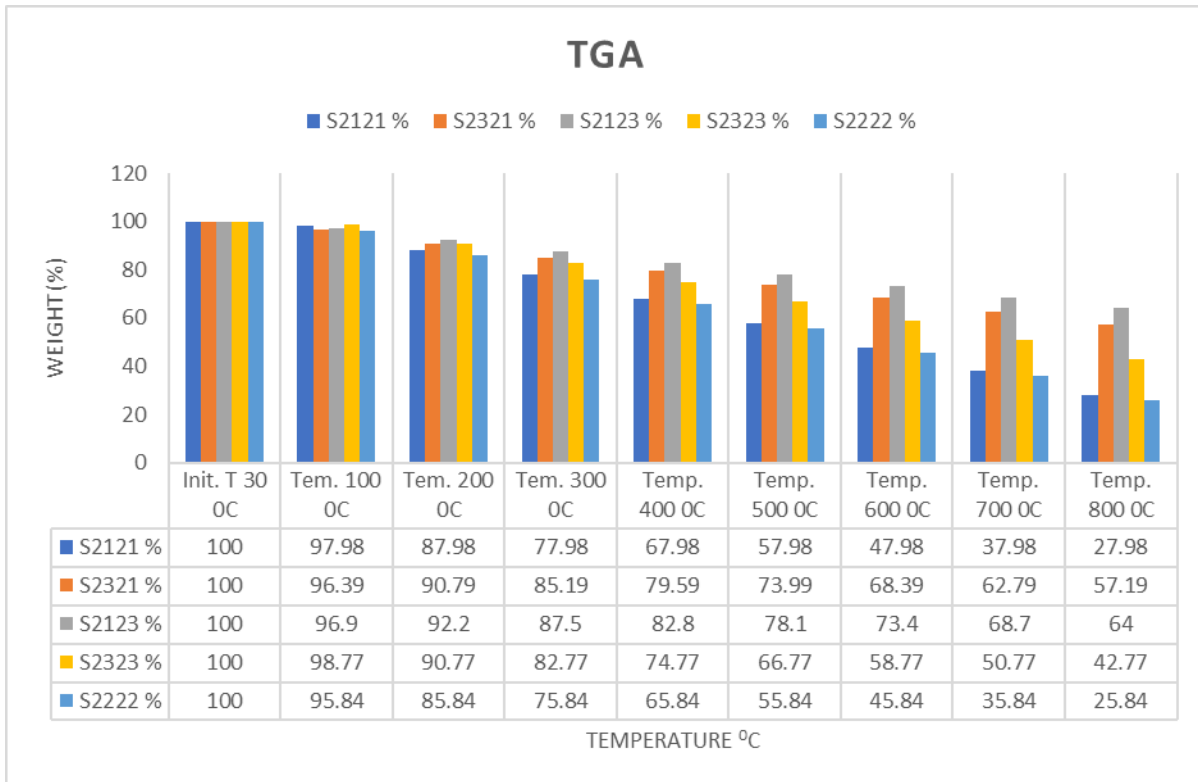


Fig. 7 TGA chart of S2121, S2321, S2123, S2323, and S2222 with variation of temperatures

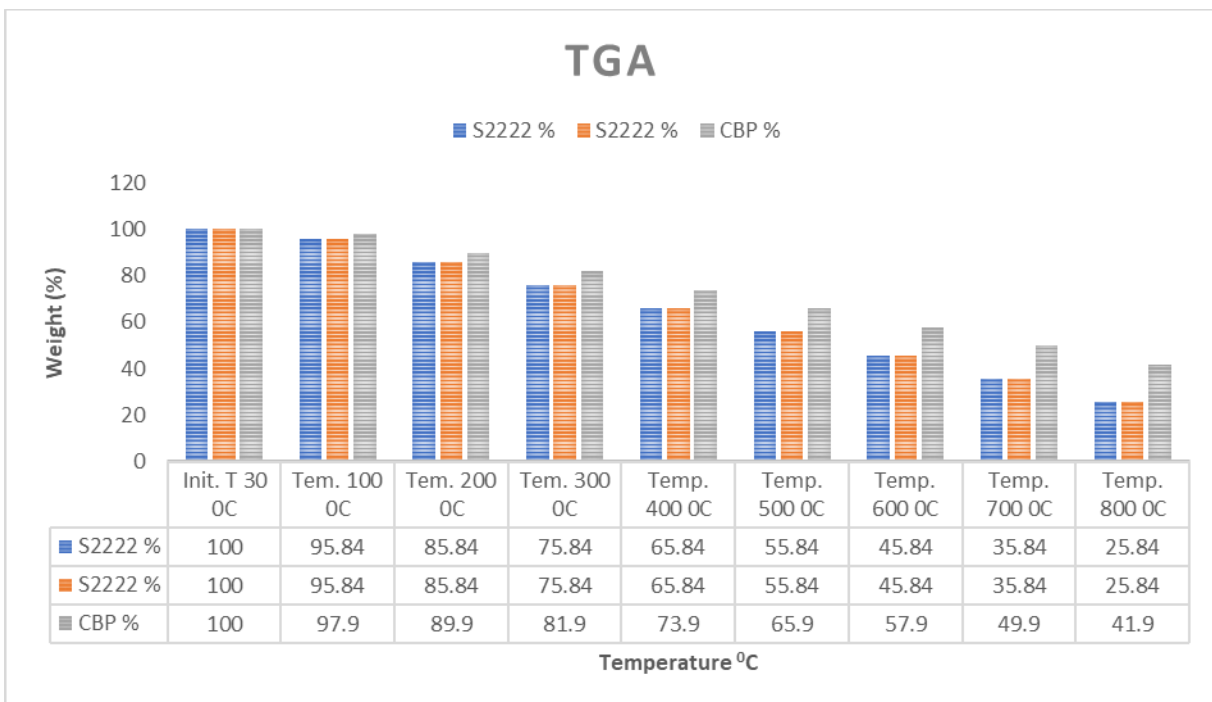


Fig. 8 TGA chart of S2222, S2222, and CBP with variation of temperatures

Table 5 Static and Dynamic Coefficient of Friction.

Specimen	Dynamic coefficient of friction (μ)			Static coefficient of friction (μ)		
	DRY DCF (μ)	Wet DCF (μ)	Oil DCF (μ)	Dry SCF (μ)	Wet SCF (μ)	Oil SCF (μ)
S1122	0.340	0.320	0.300	0.431	0.401	0.360
S3122	0.352	0.330	0.311	0.440	0.396	0.369
S1322	0.350	0.328	0.310	0.436	0.423	0.390
S3322	0.348	0.339	0.319	0.432	0.420	0.361
S2211	0.341	0.336	0.308	0.450	0.409	0.375
S2231	0.355	0.327	0.303	0.434	0.406	0.394
S2213	0.358	0.321	0.316	0.429	0.425	0.366
S2233	0.359	0.339	0.302	0.430	0.424	0.388
S1221	0.357	0.334	0.305	0.437	0.410	0.367
S3221	0.347	0.331	0.317	0.442	0.399	0.369
S1223	0.345	0.337	0.314	0.439	0.402	0.381
S3223	0.353	0.329	0.318	0.437	0.400	0.390
S2112	0.352	0.320	0.311	0.441	0.420	0.360
S2312	0.347	0.333	0.300	0.435	0.410	0.389
S2132	0.359	0.322	0.312	0.458	0.403	0.398
S2332	0.354	0.320	0.319	0.432	0.427	0.376
S1212	0.357	0.330	0.308	0.442	0.409	0.370
S3212	0.350	0.326	0.317	0.451	0.407	0.394
S1232	0.342	0.329	0.313	0.450	0.404	0.369
S3232	0.341	0.331	0.303	0.430	0.429	0.382
S2121	0.349	0.323	0.309	0.438	0.426	0.379
S2321	0.348	0.338	0.307	0.431	0.428	0.360
S2123	0.355	0.327	0.317	0.439	0.419	0.391
S2323	0.356	0.325	0.316	0.435	0.414	0.384
S2222	0.340	0.328	0.310	0.432	0.420	0.390
S2222	0.340	0.328	0.310	0.432	0.420	0.390
S2222	0.340	0.328	0.310	0.432	0.420	0.390
CBP	0.348	0.337	0.318	0.440	0.423	0.394

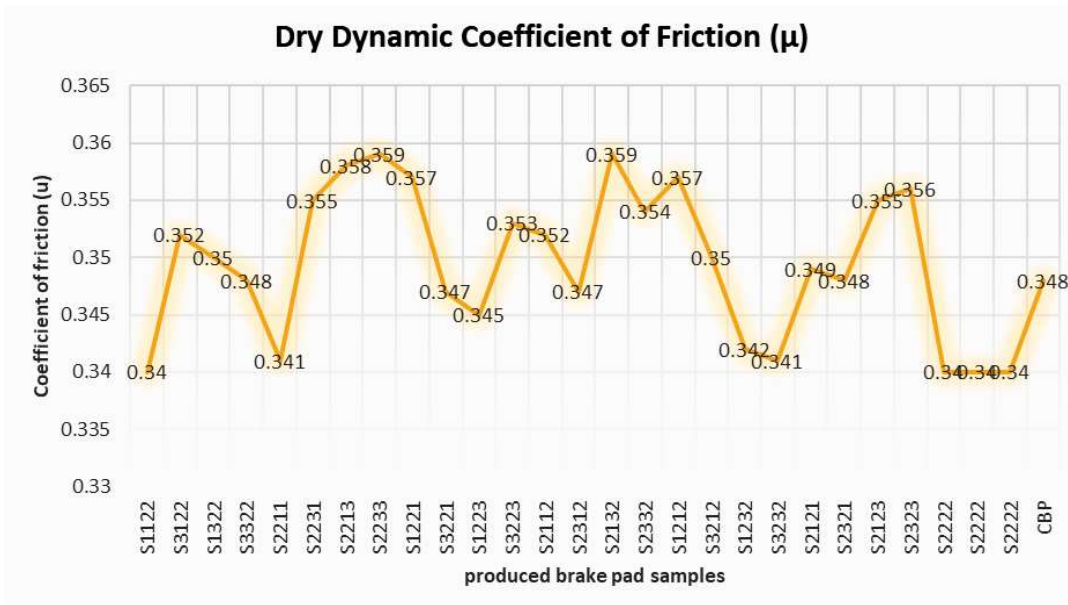


Fig. 9 Dry dynamic Coefficient of friction (μ) with the variation of produced brake pad samples

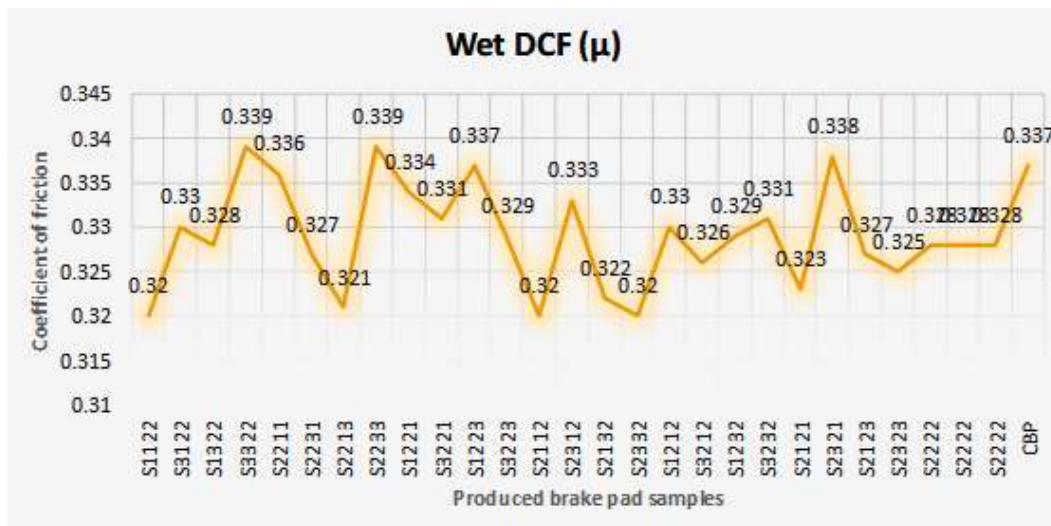


Fig. 10 Wet dynamic Coefficient of friction (μ) with variation of produced brake pad samples

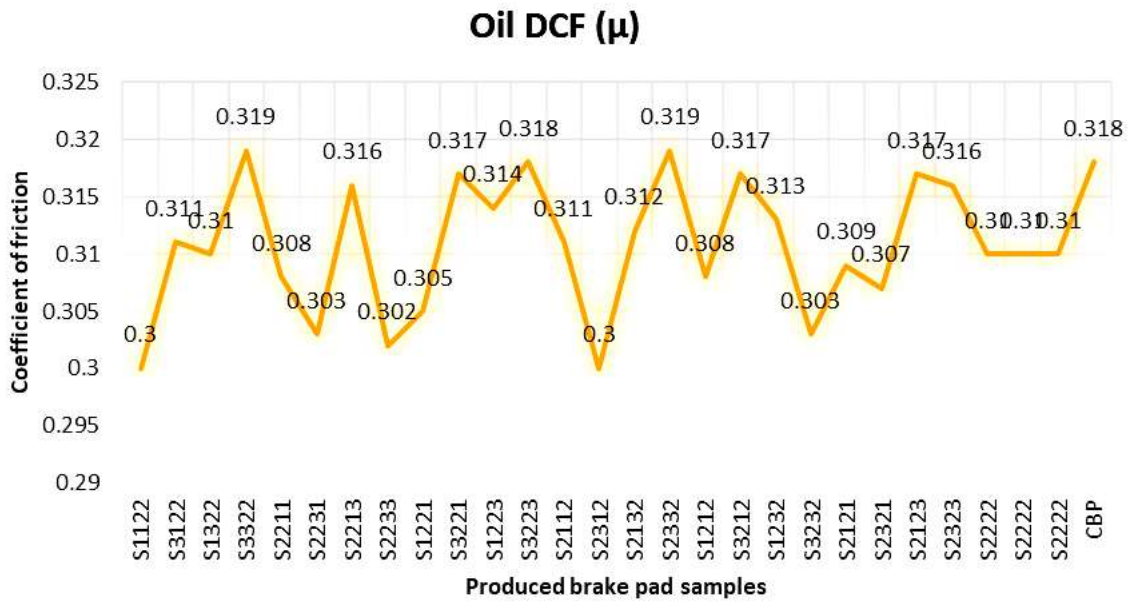


Fig. 11 Oil dynamic Coefficient of friction (μ) with variation of produced brake pad samples

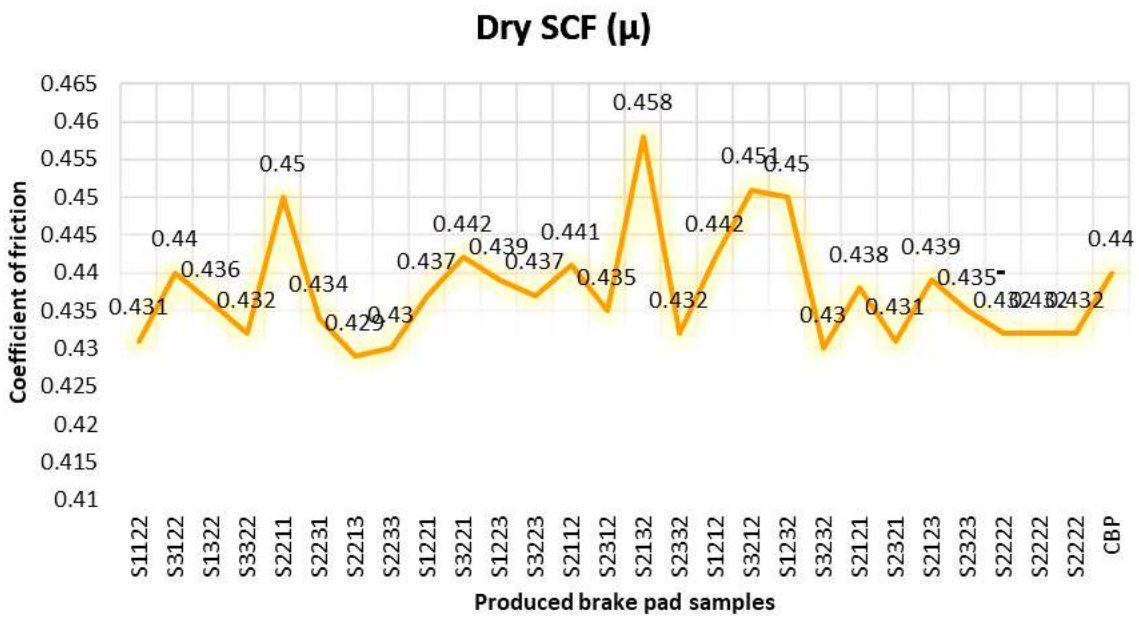


Fig. 12 Dry static Coefficient of friction (μ) with variation of produced brake pad samples

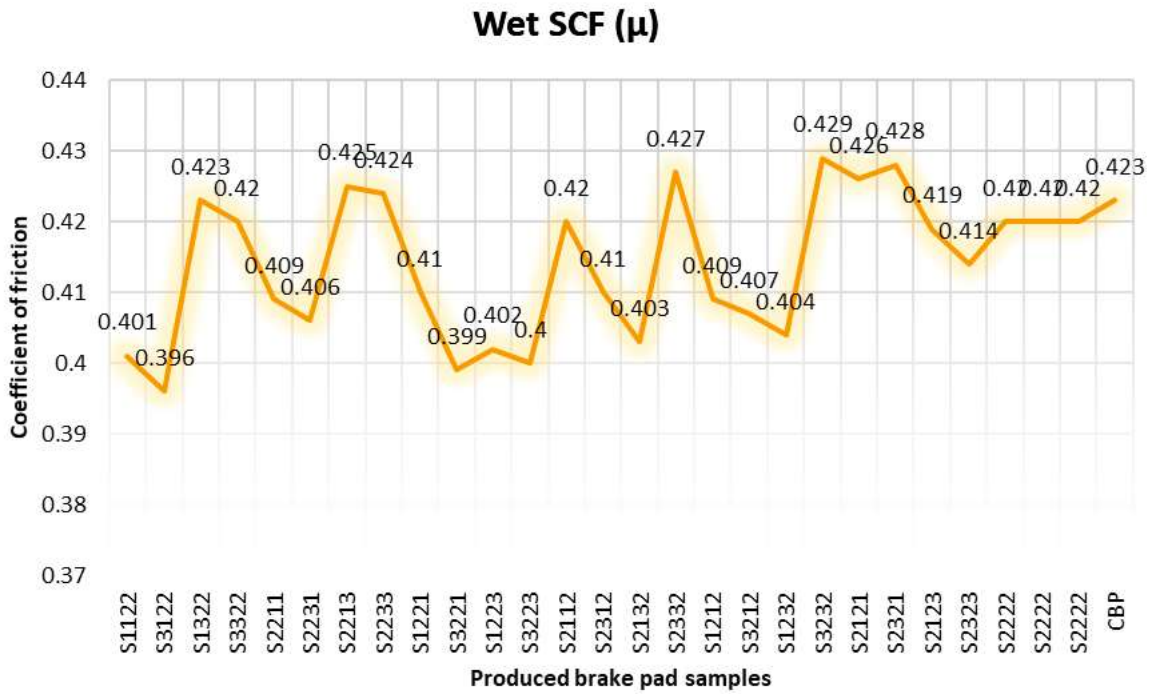


Fig. 13 Wet static Coefficient of friction (μ) with variation of produced brake pad samples

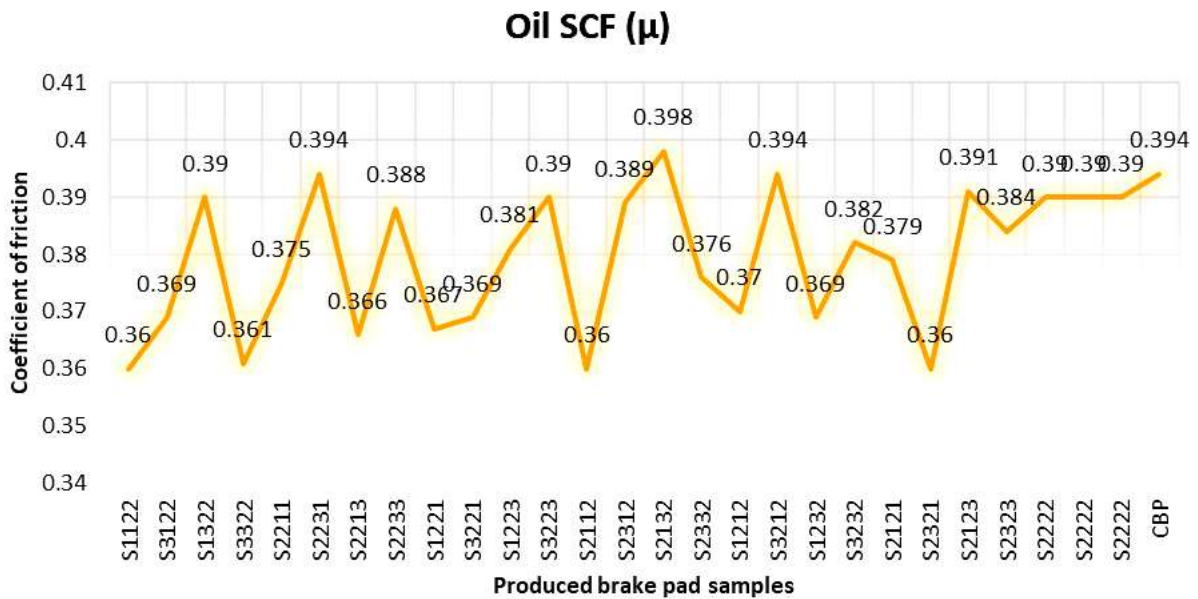


Fig. 14 Coefficient of friction μ in oil with variation of produced brake pad samples

Table 6 Rate of Wear (gram per minutes)

SAMPLES	Mass before (g)	Mass after (g)	Wear (g)	Time (minutes)	Rate of Wear (g/m)
S1122	297.23	292.70	4.530	20	0.2265
S3122	291.50	288.33	3.170	20	0.1585
S1322	281.33	279.81	3.520	20	0.076
S3322	298.90	293.65	5.250	20	0.2625
S2211	288.10	282.29	5.810	20	0.2905
S2231	290.00	287.44	4.560	20	0.1280
S2213	289.20	286.83	3.37	20	0.1185
S2233	284.22	280.67	3.550	20	0.1775
S1221	285.61	282.19	3.420	20	0.1710
S3221	299.00	290.58	8.420	20	0.4210
S1223	299.70	289.94	9.760	20	0.4880
S3223	283.40	274.45	8.950	20	0.4475
S2112	294.30	289.87	4.430	20	0.2215
S2312	286.10	280.21	5.890	20	0.2945
S2132	293.14	286.90	6.240	20	0.3120
S2332	297.53	292.26	5.270	20	0.2635
S1212	296.76	291.11	5.650	20	0.2825
S3212	298.81	293.91	4.900	20	0.2450
S1232	291.80	284.33	7.470	20	0.3735
S3232	289.11	282.89	6.220	20	0.3110
S2121	287.91	278.29	9.620	20	0.4810
S2321	292.49	286.39	6.100	20	0.305
S2123	282.65	276.45	6.200	20	0.310
S2323	285.23	281.89	3.340	20	0.167
S2222	297.52	291.39	6.130	20	0.3065
S2222	297.52	291.39	6.130	20	0.3065
S2222	297.52	291.39	6.130	20	0.3065
CBP	291.10	298.22	3.920	20	0.356

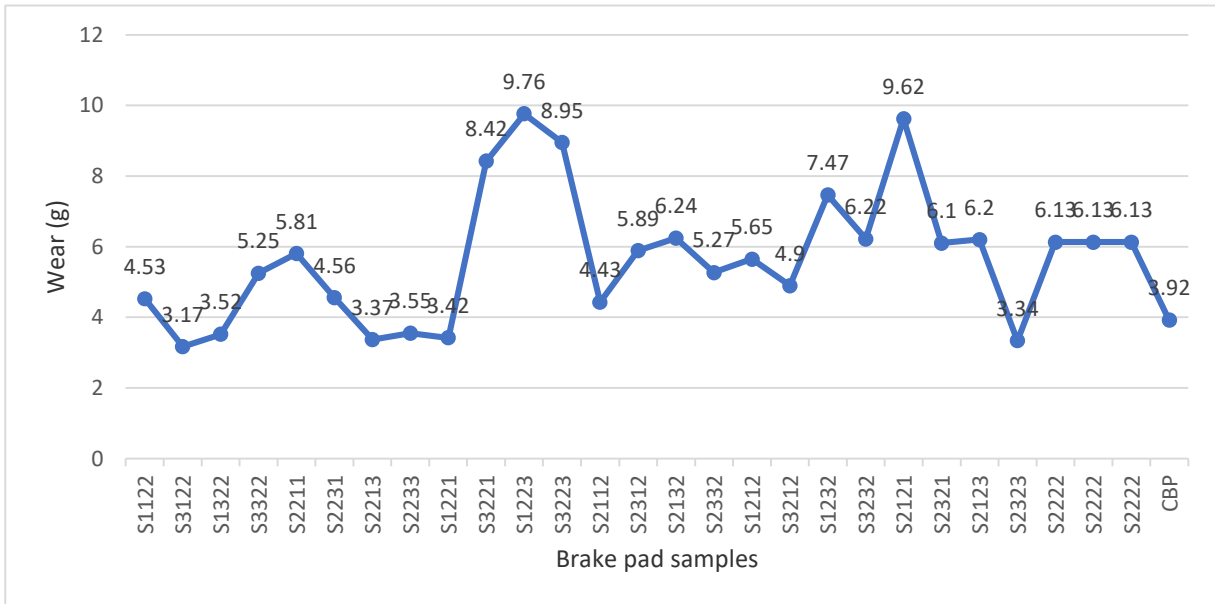


Figure 15. Graph of Brake Pad Samples Wear (g)

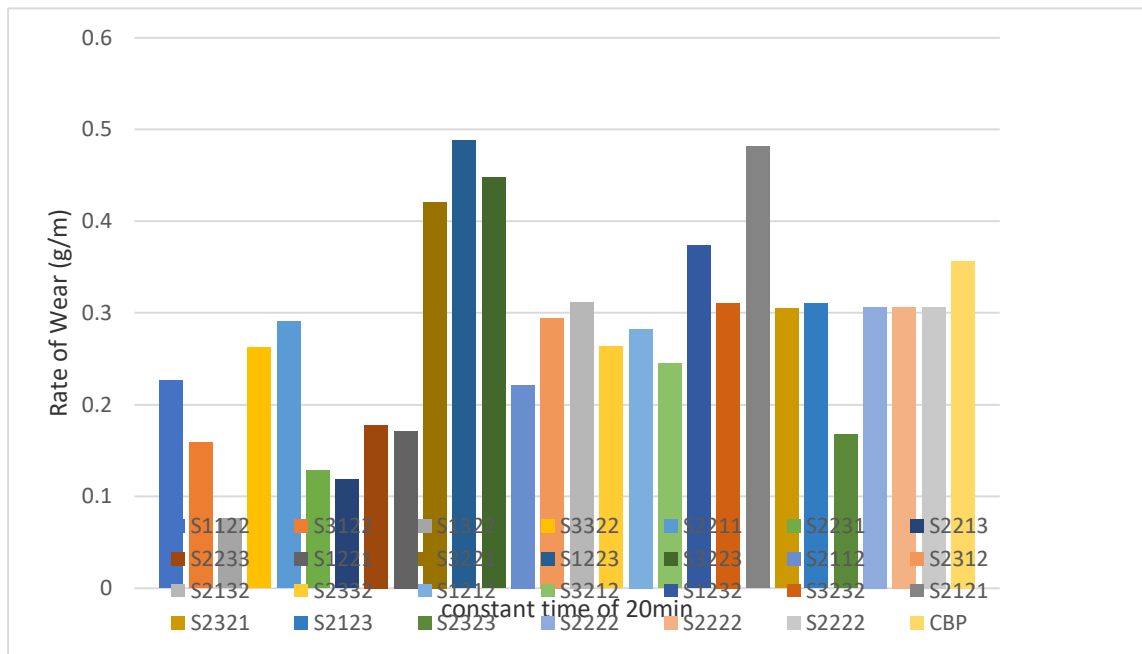


Fig. 16 Graph of Brake Pad Samples rate of wear (g/m)

3.2 Characterization of Wear and Wear Rate

Figure 4.11 and 4.12 shows the variation of wear and wear rate with constant speed and time of 150rpm and 18min. For brake pads produced from CFF

and OSS alongside with the commercial brake pad (CBP). Wear and Wear rate data varies for different formulations due to unlike additives and their weight

percentages used in their compositions. The contact pressure (74KN/m²) between the rotor and brake pads with constant speed and time led to the variation in friction pad samples produced. The trend was reported by [13-14]. The minimum produced brake pad (S3122) wear was 3.17g while that of commercial brake pad was 3.92g as shown in Fig. 4. In sequential order, from minimum to maximum, the produced brake pad and commercial brake pad wear are S3122 – 3.17g, S2323 – 3.34g, S2213 – 3.37g, S1221 – 3.37g, S1322 – 3.52g, S2233 – 3.55g, CBP – 3.92g, S2112 – 4.43g, S1122 – 4.53g, S2231 – 4.56g, S3212 – 4.90g, S3322 – 5.25g, S2332 – 5.27g, S1212 – 5.65g, S2211 – 5.81g, S2312 – 5.89g, S2321 – 6.10g, S2222 – 6.13g, S2222 – 6.10g, S2222 – 6.10g, S2123 – 6.20g, S3232 – 6.22g, S2132 – 6.24g, S1232 – 7.47g, S3221 – 8.42g, S3223 – 8.95g, S2121 – 9.62g, and S1223 – 9.76g. Sample S3122 – 3.17g, exhibited less wear rate than commercial brake pad CBP – 3.92g. These wear rates were better than the 4.20 and 4.40g values described by [15-16]. The lowest values of wear rate obtained from the produced friction pads could be attributed to the type of binder (phenolic resin) used, and it is evident that the phenolic resin used for the formulation of the pads provides a better bonding of the friction materials that resist wear rates.

4. Conclusion

In conclusion, all the characteristics of the brake pad produced are superior to the commercial brake pad due to its additive use that gives better bonding, low wear, and low thermogravimetric analysis. Hence, these produced samples of friction lining can be recommended to the society of automobile engineering SAE for use in brake pad application.

Acknowledgement

The authors would like to thank all those who have contributed in one way or another to the success of this work. Mentioned here are just a few, the Mechanical Workshop, Federal University of Technology, Minna. Engineering Workshop, Federal Polytechnic Kaduna, Kaduna State Nigeria, School of science laboratory technology and University of Port-Harcourt, Nigeria.

References

1. R.O. Edokpia et al., "Experimental study of the properties of brake pad using eggshell particles-Gum Arabic composites," *Journal of the Chinese Advanced Materials Society*, vol. 4, pp. 172-184, 2015.
2. J. Kukutschová et al., "Wear performance and wear debris of semi-metallic automotive brake materials," *Wear*, vol. 268, pp. 86-93, 2010.
3. C. Pinca-Bretotean et al., "Laboratory testing of brake pads made of organic materials intended for small and medium vehicles," *Materials Science and Engineering*, vol. 393, pp. 1-7, 2018.
4. D.-A. Bashar et al., "Material selection and production of a cold-worked composite brake pad," *World J. Eng. Pure Appl. Sci.*, vol. 2, pp. 96, 2012.
5. R. Yun et al., "Application of extension evaluation method in development of novel eco-friendly brake materials," *SAE Int J Mater Manuf*, vol. 2, pp. 1-7, 2010.
6. J.P. Blau, "Compositions, functions and testing of friction brake materials and their additives. A report by Oak Ridge National Laboratory for U.S. Dept. of Energy 2001, 78-80." [Online]. Available: <http://www.Ornl.gov/webworks/cpr/y2001/rpt/112956.pdf> [February 2015].
7. S.J. Eziwhuo et al., "Evaluation of apricot kernel, avocado and African pear seed oils as vegetable-based cutting fluids in turning AISI 1020 steel," *IOSR Journal of Engineering (IOSRJEN)*, vol. 09, no. 3, pp. 10-19, March 2019.
8. D. Chan and G.W. Stachowiak, "Review of automotive brake friction materials," *Proc Inst Mech Eng Part D J Automob Eng*, vol. 218, pp. 953-966, 2004.
9. B.D. Garg et al., "Brake wear particulate matter emissions," *Environ Sci Technol*, vol. 34, pp. 4463-4469, 2000.
10. A. Borawski, "Suggested research method for testing selected tribological properties of friction components in vehicle braking systems," *Acta Mechanica et Automatica*, vol. 10, no. 3, pp. 223-226, 2016.
11. K. Kulikowski and D. Szpica, "Determination of directional stiffnesses of vehicles' tires under a static load operation," *Maintenance and Reliability*, vol. 16, no. 1, pp. 66-72, 2014.
12. J. Wahlstrom, "Towards a simulation methodology for prediction of airborne wear particles from disc brakes: licentiate thesis. Department of Machine Design, Royal Institute of Technology, Stockholm, ISBN 978-91-7415-391-0," 2009.
13. C.V. Ossia and A. Big-Alabo, "Development and characterization of green automotive brake pads from waste shells of giant African snail (*Achatina achatina* L.)," *The International Journal of Advanced Manufacturing Technology*, vol. 2021, [Online]. Available: <https://doi.org/10.1007/s00170-021-07085-4>.
14. S.J. Eziwhuo and T. Joseph, "Performance evaluation of non-edible vegetable seed oil as cutting fluid in metal turning operation," *World Journal of Engineering Research and Technology (WJERT)*, vol. 6, no. 4, pp. 354-366, 2020.
15. T. Mutuk and M. Gurbuz, "Effect of pure titanium particle size on density, hardness, wear resistance, and microstructure properties," *Journal of Metals, Materials and Minerals (JMMM)*, vol. 29, no. 03, pp. 54-59, 2019.
16. J. Abutu et al., "Production and characterization of brake pad developed from coconut shell reinforcement material using central composite design," *SN Applied Sciences*, vol. 1, no. 18, 2019.